Environmental Technology
Publication details, including instructions for authors and subscription information:
http://www.tandfonline.com/loi/tent20

Hybrid materials from agro-waste and nanoparticles: implications on the kinetics of the adsorption of inorganic pollutants

Martins O. Omorogie[ab], Jonathan O. Babalola[b], Emmanuel I. Unuabonah[cd] & Jian R. Gong[a]

[a] National Center for Nanoscience and Technology (NCNST), Beijing, People's Republic of China

[b] Department of Chemistry, University of Ibadan, Ibadan, Nigeria

[c] Department of Chemical Sciences, Redeemer's University, P.M.B. 3005, Mowe, Nigeria

[d] Institüt fur Chimie, Universität Potsdam, Germany

Published online: 01 Oct 2013.

To cite this article: Martins O. Omorogie, Jonathan O. Babalola, Emmanuel I. Unuabonah & Jian R. Gong (2014) Hybrid materials from agro-waste and nanoparticles: implications on the kinetics of the adsorption of inorganic pollutants, Environmental Technology, 35:5, 611-619, DOI: 10.1080/09593330.2013.839747

To link to this article: http://dx.doi.org/10.1080/09593330.2013.839747

Environmental Technology, 2014
Vol. 35, No. 5, 611–619, http://dx.doi.org/10.1080/09593330.2013.839747

Taylor & Francis
Taylor & Francis Group

Hybrid materials from agro-waste and nanoparticles: implications on the kinetics of the adsorption of inorganic pollutants

Martins O. Omorogie[a,b], Jonathan O. Babalola[b], Emmanuel I. Unuabonah[c,d*] and Jian R. Gong[a*]

[a]*National Center for Nanoscience and Technology (NCNST), Beijing, People's Republic of China;* [b]*Department of Chemistry, University of Ibadan, Ibadan, Nigeria;* [c]*Department of Chemical Sciences, Redeemer's University, P.M.B. 3005, Mowe, Nigeria;* [d]*Institüt fur Chimie, Universität Potsdam, Germany*

(*Received 10 May 2013; final version received 25 August 2013*)

This study is a first-hand report of the immobilization of *Nauclea diderrichii* seed waste biomass (ND) (an agro-waste) with eco-friendly mesoporous silica (MS) and graphene oxide–MS (GO + MS) nanoparticles, producing two new hybrid materials namely: MND adsorbent for agro-waste modified with MS and GND adsorbent for agro-waste modified with GO + MS nanoparticles showed improved surface area, pore size and pore volume over those of the agro-waste. The abstractive potential of the new hybrid materials was explored for uptake of Cr(III) and Pb(II) ions. Analysis of experimental data from these new hybrid materials showed increased initial sorption rate of Cr(III) and Pb(II) ions uptake. The amounts of Cr(III) and Pb(II) ions adsorbed by MND and GND adsorbents were greater than those of ND. Modification of *N. diderrichii* seed waste significantly improved its rate of adsorption and diffusion coefficient for Cr(III) and Pb(II) more than its adsorption capacity. The rate of adsorption of the heavy metal ions was higher with GO + MS nanoparticles than for other adsorbents. Kinetic data were found to fit well the pseudo-second-order and the diffusion–chemisorption kinetic models suggesting that the adsorption of Cr(III) and Pb(II) onto these adsorbents is mainly through chemisorption mechanism. Analysis of kinetic data with the homogeneous particle diffusion kinetic model suggests that particle diffusion (diffusion of ions through the adsorbent) is the rate-limiting step for the adsorption process.

Keywords: adsorption; graphene oxide; nanoparticles; kinetic models; hybrid materials

1. Introduction

The upsurge of global industrialization has led to elevated pollution problems that are threatening the health of man. Various industries including the petroleum refineries, tanneries, textile industries, chrome plating industries, steel industries and other manufacturing industries release some of these heavy metal ions into the environment.[1]

These heavy metals are carcinogenic and mutagenic.[1] Chromium is known to be essential to animals and plants and plays an important role in sugar and fat metabolism, although in excess can cause allergic skin reactions and cancer.[2] Lead bioaccumulation in the body over a long period of time can cause damage to the arteries, kidney, liver and reproductive system, and cause nervous/brain disorder in children.[3]

Currently, there is an intense search for cheap, ubiquitous and cost-effective materials for the removal of toxic metals from industrial wastewaters and polluted water, especially those of agricultural origin.

Nauclea diderrichii seed waste biomass (ND) is relatively abundant and ubiquitous in the humid tropical rainforest zone of south-western Nigeria.[4,5] Researchers have exploited various adsorbents for the sequestration of Cr(III), Cd(II), Hg(II), Cr(VI), Cu(II) and Zn(II) in past studies.[6–12]

Agro-materials are known to have abundant content of lignocellulose, which essentially impacts high removal efficiency of toxic metal ions (inorganic pollutants) and even recalcitrant toxic organic pollutants such as polyaromatic hydrocarbons (PAHs) and polychloro biphenyls (PCBs).[13,14] However, the use of agro-wastes as biosorbents has a drawback known as 'bleeding' resulting from biodegradation of the biomass (agro-waste) when left in solution from few hours to days.[14] Furthermore, some agro-wastes do not have the appropriate bulk densities for industrial applications. Thus, these have limited the use of agro-wastes to the laboratory.

Mesoporous materials have been applied in surface processes like catalysis, photocatalysis, advance oxidation processes and adsorption.[15–18] In recent times, functionalities have been grafted to the surfaces of various mesoporous nanomaterials, including functionalized graphene oxide (GO) nanoparticles to selectively adsorb various pollutants of interest to researchers.[19–21]

However, GO nanoparticles and mesoporous materials are expensive and are thus not cost-effective as adsorbents

*Corresponding authors. Emails: iyaemma@yahoo.com, gongjr@nanoctr.cn

for removal of micropollutants from aqueous solutions. It is, however, thought that modifying GO and mesoporous silica (MS) nanoparticles with cheap materials rich in functionalities will reduce their costs without compromising their efficiency to remove micropollutants from aqua systems.

It is in this vein that this study reports, for the first time the implications of modifying an agro-waste with MS and GO nanoparticles to produce a new class of hybrid materials relevant for the removal of toxic metal ions from the aqua system. This modification was aimed at improving the surface properties of ND and thus its adsorption capacity for toxic metal ions of interest.

2. Experimental details

2.1. Preparations of ND, MS, GO, MND and GND adsorbents

ND was obtained from the Forest Research Institute of Nigeria (FRIN), in Ibadan (7°23′16″ north, 3°53′47″ east), Nigeria. After collection, it was heated at 60 °C for 3 h. Thereafter, it was pulverized and sieved to 450 μm particle size which was used for this research.

MS nanoparticles were prepared by the liquid templating method as described by Kresge et al.[15] One gram of cethyl trimethyl ammonium bromide (CTAB – 99% purity) was weighed and dissolved in 480 mL deionized water. Thereafter, 3.5 mL of 2 M NaOH – 99% purity was added to CTAB/H_2O solution. The beaker containing CTAB/H_2O solution was immersed in a silicone oil bath and was heated with an electric heater to 80 °C. The reaction mixture was agitated continuously at 1000 rpm for 1 h. Thereafter, 6 mL of triethyl ortho silicate (TEOS) (99% purity) was added drop wise to the reaction mixture and further heated for 2 h at 80 °C. After cooling, the white precipitate formed was separated from the suspension using a separating funnel under vacuum. The white precipitate obtained was dried in an oven for 3 h at 100 °C before being calcined for 5 h at 550 °C.[15]

GO nanoparticles were synthesized by chemical oxidation of natural graphite flake according to the method described by Hummers and Offeman.[22] Concentrated sulphuric acid – 98% purity and orthophosphoric acid – 85% purity (400:50 mL) were added to a mixture of $KMnO_4$ – 99.3% purity (30 g) and graphite – 95% purity (5 g). It was heated to 50 °C and stirred for 24 h. The resulting mixture was poured into ice (250 mL) and H_2O_2 – 50% purity (30%, 50 mL) and then filtered using a polycarbonate membrane. The solid product, GO, was washed with water, 30% HCl – 36% purity and ethanol for two times before vacuum drying for 12 h using the vacuum dessicator.

The MS nanoparticles prepared initially were subsequently added to ND in simple ratio and then added to a 1 L beaker containing 500 mL milli-Q deionized water. This reaction mixture was agitated at 1250 rpm at 20 °C for 48 h and the agro-waste–MS hybrid material (MND adsorbent) was filtered via vacuum filtration. The wet MND adsorbent was placed in a heating crucible and dried at 100 °C overnight. A portion of the MND hybrid material was weighed into plastic containers and kept for adsorption studies.

Thereafter, GO, MS and ND in simple ratio were placed in a 1 L beaker containing 700 mL milli-Q deionized water. The reaction mixture was agitated for 48 h at 20 °C and 1000 rpm. The agro-waste–GO–MS hybrid material (GND) was also filtered by vacuum filtration and the wet GND hybrid material was placed in a heating crucible and dried at 100 °C overnight. The GND hybrid material was weighed into plastic containers and kept for adsorption studies.

2.2. Physicochemical characterizations of ND, MS, GO, MND and GND materials

Various physicochemical characterizations of the ND, GO nanoparticles, MS nanoparticles, ND modified with MS nanoparticles (MND) adsorbent and ND modified with GO–MS nanoparticles (GND) adsorbent were carried out using the Perkin Elmer Spectrum 1 Fourier Transform Infrared (FTIR) spectrometer in conjunction with KBr wafer, nitrogen sorption–desorption at 77 K was carried out using the specific surface area/porosity analyser, Micromeritics Instrument Corporation, ASAP 2020 Model analyser (for specific surface area analysis), X-ray Diffractometer (XRD) (D/Max-2500, Rigaku, Japan) with Cu Kα radiation and Perkin Elmer Thermogravimetric/differential thermal analyser (TG), scanning electron microscope (SEM) (Hitachi S4800 Model) and transmission electron microscope (TEM) (F20 S-TWIN, Tecnai G2, FEI Co.).

2.3. Adsorption study

Fifty milligrams each of ND agro-waste, MND and GND adsorbents were added to 20 mL of 20 mg/L Cr(III) and Pb(II) solutions prepared from $Cr(NO_3)_3{\cdot}9H_2O$ and $Pb(NO_3)_2$ salts, respectively. The suspensions were agitated in a reciprocal shaker within a time range of 5–60 min. Samples were withdrawn at various time intervals and filtered using filter papers. The supernatants obtained were analysed for residual Cr(III) and Pb(II) ions, using the inductively coupled plasma-optical emission spectrometer and the Perkin Elmer Optima 5300DV Model.

The experimental data obtained from this study were fitted into four kinetic models; pseudo-first-order (PFO),[23,24] pseudo-second-order (PSO),[24,25] diffusion–chemisorption (DC) [26] and homogeneous particle diffusion (HPD) [27,28] models with their respective linearized and non-linearized mathematical expressions given as follows.

Pseudo-first-order model

$$\ln(q_e - q_t) = \ln q_e - k_1 t, \tag{1}$$

$$q_t = q_e\,(1 - \exp(-k_1 t)). \tag{2}$$

Pseudo-second-order model

$$\frac{t}{q_t} = \frac{t}{q_e} + \frac{1}{k_2 q_e^2}, \tag{3}$$

$$q_t = \frac{k_2 q_e^2 t}{1 + k_2 q_e t}, \tag{4}$$

where q_e is the amount of metal ion adsorbed by the adsorbent (mg/g), q_t is the amount of metal ion adsorbed at time t (min) by the adsorbent (mg/g) and k_1 and k_2 are the PFO (min^{-1}) and PSO ($g\,mg^{-1}\,min^{-1}$) model rate constants, respectively.

Also, the initial adsorption rate h (mg g/min) is given below as

$$h = k_2 q_e^2. \tag{5}$$

2.3.1. *Diffusion-chemisorption model*

An empirical Diffusion-chemisorption (DC) kinetic model was developed by Sutherland and Venkobachar [26] to simulate the adsorption of toxic metal ions onto heterogeneous media. The differential form of this model is given as

$$\frac{dq_t}{dt} = \frac{nK_{DC}t^{n-1}}{q_e^2}(qe - qt)^2, \tag{6}$$

where q_t is the amount of adsorbate on the adsorbed per time (mg/g), K_{DC} is the rate of mass transfer of adsorbate ($mg/g\,t^{0.5}$), q_e is the equilibrium adsorption capacity of the adsorbent (mg/g) and t is the time (min).

Separating the variables in Equation (6) gives

$$\frac{q_e^2\,dq_t}{(q_e - q_t)^2} = nK_{DC}\,dt \times t^{n-1}. \tag{7}$$

For the boundary conditions $t = 0$ to $t = t$ and $q_t = 0$ to $q_t = q_t$, the integrated form of Equation (7) becomes

$$\frac{q_e^2}{(q_e - q_t)} = K_{DC}t^n + q_e. \tag{8}$$

Rearranging Equation (8) and substituting this value of n in the above equation produced the nonlinear form below:

$$q_t = \frac{1}{1/q_e + 1/K_{DC}t^{0.5}}. \tag{9}$$

However, according to Haerifar and Azizian,[29] the values of n which is the kinetic rate coefficient could also be 1 or 2. For $n = 1$ the PFO kinetic model is employed indicating that the change of adsorbate concentration in aqueous solution is small or the relative surface coverage is very negligible. This condition is valid at initial adsorption times or close to equilibrium. For $n = 2$, the PSO kinetic model suggests that the change of adsorbate concentration is observable.[29]

Rearrangement of Equation (9) will give the linear form below:

$$\frac{t^{0.5}}{q_t} = \frac{t^{0.5}}{q_e} + \frac{1}{K_{DC}}. \tag{10}$$

2.3.2. *Homogeneous particle diffusion model*

In the homogeneous particle diffusion model, the medium is seen as homogeneous and gel like. The solute is adsorbed at the particle surface and diffuses towards the centre in a process governed by a driving force due to a gradient in the adsorbed solute concentration, and a diffusion coefficient.[27] In this model, the rate-determining step is usually described by either (i) diffusion of ions through the liquid film surrounding the particle, called the film diffusion or (ii) diffusion of ions into sorbent beads called particle diffusion mechanism.[28] Using the Fickian equation to describe the diffusion rate constant, we have;

$$X(t) = 1 - \frac{6}{\pi^2}\sum_{Z=1}^{\infty}\frac{1}{Z^2}\exp\left[\frac{-Z^2\pi^2 D_e t}{r^2}\right]. \tag{11}$$

Equation (11) was approximated to (12), that is called Vermeulen equation [30] and this was used to fit a range $0 < X(t) < 1$ for the adsorption controlled by particle diffusion,[30]

$$X(t) = \left[1 - \exp\left[-\frac{\pi^2 D_e^2 t}{r^2}\right]\right]^{1/2}. \tag{12}$$

The above equation can be expressed as;

$$-\ln(1 - X^2(t)) = 2Kt,$$

where $K = \pi^2 D_e/r^2$.

If liquid film diffusion controls the rate of adsorption, the following analogous expression can be used:

$$X(t) = 1 - \exp\left[\frac{3D_e C}{r\delta C_r}\right], \tag{13}$$

$$-\ln(1 - X(t)) = K_{Li}t, \tag{14}$$

where $K_{Li} = 3D_eC/r\delta C_r$,

$X(t)$ is the fractional attainment of equilibrium at time $t = q_t/q_e$; D_e, the effective diffusion coefficient of sorbates in the sorbent phase ($m^2\,s^{-1}$); r, the radius of the adsorbent particle assumed to be spherical (m); Z, the integer; C, the total concentration of both exchanging species, M; C_r, the total concentration of both exchanging species in the ion exchanger, M; K_{Li}, the rate constant for film diffusion (infinite solution volume condition); and δ, the thickness of liquid film.

3. Results and discussion

3.1. *Physicochemical characterizations*

3.1.1. *FTIR spectroscopy*

Figure 1(a) and 1(b) shows the FTIR spectra of ND agro-waste, MS nanoparticles, MND and GND adsorbents, and GO nanoparticles, respectively.

The FTIR spectrum of ND has been previously described by Omorogie et al.[7] The FTIR spectrum of MS nanoparticles showed a broad peak at 3400 cm^{-1} which is

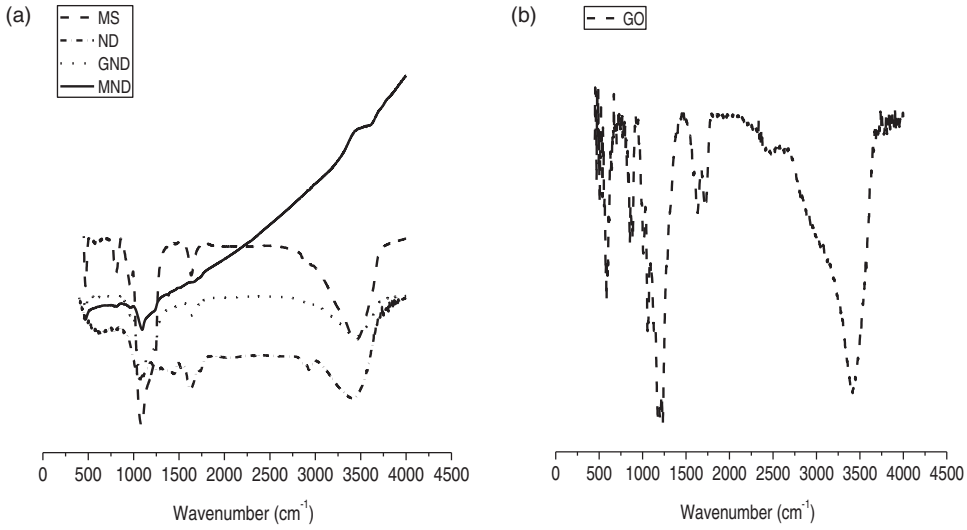

Figure 1. FTIR spectra of (a) MS nanoparticles, ND agro-waste, GND and MND adsorbents and (b) GO nanoparticles.

assigned to the −OH of silanol.[31] The peak at 2900 cm^{-1} is assigned to −C−H of $-CH_2$ and $-CH_3$ of aliphatic chains of the Si precursor.[32] The peak at 1730 cm^{-1} is assigned to the $R-NH_3^+$ group found likely in trace of surfactant left in MS after calcination.[33] The 1210 and 920 cm^{-1} absorption bands are assigned to −Si−O− and −Si−O−Si− bending vibrations, respectively, which are from the silica framework (Figure 1(a)).[31,34,35]

The FTIR spectrum of GO nanoparticles showed peaks at 3500, 1760–1720, 1240–1230 and 1050 cm^{-1} which are assigned to −OH stretch, −C=O stretch, −C−O stretch and −C−O bend vibrations, respectively (Figure 1(b)).[21]

The MND adsorbent spectrum indicates that the broad peak at 3400 cm^{-1} in MS nanoparticles disappeared, probably due to the formation of hydroxylated compounds [36] during the preparation of this hybrid material. The peak at 1700 cm^{-1} is assigned to −C=O of carboxylate group.[37] The −Si−O− absorption band gave a significant shift from 1210 to 1100 cm^{-1} with the disappearance of the 920 cm^{-1} suggesting the possibility of MS hybrid material interacting with the hydroxyl groups on ND.

The GND adsorbent spectrum showed peaks that were observed at 3500, 2900, 1730, 1450, 1205 and 805 cm^{-1} (Figure 1(a)) which indicates the presence of −OH stretch, −C−H stretch of $-CH_2$ and $-CH_3$, −C=O stretch, −C=C− stretch, −C−O stretch and −C−C− or −C−H out-of-plane bending vibration, respectively, in the GND adsorbent.[37]

The presence of −C=O stretch in both hybrid materials and the −C=C− and −C−H stretch in GND adsorbent suggests the presence of ND in both of them.

3.1.2. *Brunauer–Emmett–Teller (BET) nitrogen sorption–desorption at 77 K*

Table 1 shows data for the nitrogen sorption–desorption plots at 77 K for ND, MND and GND hybrid materials.

Table 1. Nitrogen sorption–desorption at 77 K data for ND agro-waste, MS nanoparticles, GO nanoparticles, MND and GND adsorbents.

	ND	MS	GO	MND	GND
Single point surface area at P/P_0 (m^2/g)	2.532	749.944	26.782	199.099	253.107
BET surface area (m^2/g)	5.357	789.746	25.386	209.474	266.600
Langmuir surface area (m^2/g)	21.265	1098.335	33.702	294.628	372.454
T-plot external surface area (m^2/g)	7.454	1024.251	28.326	268.945	337.314
BJH adsorption cumulative surface area of pores (m^2/g)	6.341	964.042	23.95	240.563	295.227
Single point adsorption total pore volume of pores (cm^3/g)	0.00404	0.751	0.018	0.243	0.291
BJH adsorption cumulative volume of pores (cm^3/g)	0.00632	1.118	0.081	0.446	0.546
BET adsorption average pore width (nm)	3.014	3.804	2.814	4.631	4.365
BJH adsorption average pore width (nm)	3.985	4.639	13.48	7.422	7.397

Note: BJH, Barett–Joyner–Halenda.

The specific surface area, pore volume and pore size of ND increased from 5.36 to 209.5 m^2/g, 0.006 to 0.446 cm^3/g and 3.985 to 7.422 nm, respectively, in the MND adsorbent

while in GND adsorbent, they increased to 266.6 m^2/g, 0.546 cm^3/g and 7.397 nm, respectively (Table 1). These increases in the surface properties of ND are due to its immobilization on MS and GO nanoparticles, which already have very high specific surface area, pore volume, pore size and extra functional groups.[16–18]

3.1.3. *Thermogravimetry and differential thermal analysis TG/DTA*

TG analysis (Figure 2(a)) suggests that MS nanoparticles showed only weight loss (ca. 6%) from 80 °C to 1000 °C which may be attributed to loss of surface water, solvent and cationic surfactant.[38]

The TG analysis of ND (Figure 2(a)) was described by Omorogie et al. [7] in our previous work.

However, MND adsorbent (Figure 2(a)) showed that weight losses of ca. 9% from 50 °C to 100 °C and ca. 41% from 100 °C to 600 °C are attributed to loss of surface water [39] and loss of cationic surfactant and thermal decomposition of cellulosics/lignin, respectively.

The GO nanoparticles (Figure 2(a)) showed weight losses of ca. 11% from 20 °C to 200 °C and ca. 70% from 250 °C to 900 °C due to loss of surface water, solvent and decomposition of the carbon-based precursor.[38]

The GND adsorbent showed weight losses of ca. 10% from 20 °C to 250 °C and ca. 40% from 250 °C to 650 °C owing to loss of surface water and cationic surfactant and decomposition of volatile matter with some decomposition of cellulosics/lignin (Figure 2(a)).

Differential thermal analysis (DTA) (Figure 2(b)) showed two exothermic peaks (ca. 380 °C and 440 °C) for MND adsorbent, confirming the heat release from loss of surface water, cationic surfactant and thermal decomposition of volatile organic matter and cellulosics/lignin as earlier observed with TG analysis.[31]

The DTA of ND (Figure 2(b)) was described by Omorogie et al. [7] in our previous work. From DTA (Figure 2(b)), two endothermic peaks (ca. 50–350 °C and 650–800 °C) are attributed to heat absorbed in two stages by GO nanoparticles. This is due to the high thermal conductivity of GO nanoparticles at low and very high temperatures.[19] Also, two exothermic peaks (ca. 350–650 °C and > 800 °C) were observed for GO, due to heat losses in two stages as a result of carbon burn off.[19] The DTA for MS nanoparticles (Figure 2(b)) showed one endothermic peak from 0 to 350 °C which confirmed the loss of surface water and the exothermic peak at ca.350 °C which also confirmed the loss of cationic surfactant.[38] The GND hybrid material showed an endothermic peak (50–500 °C) due to heat losses from surface water, surfactant, volatile organic matter and decomposition of cellulosics/lignin, confirming TG analysis for GND hybrid material.[31]

3.1.4. *X-ray diffractometry*

The XRD patterns of MS, MND hybrid material and ND are shown in Figure 3(a) and those for GO nanoparticles and GND adsorbent are shown in Figure 3(b). The XRD pattern of MS nanoparticles gave a very sharp peak at $2\theta = 5.2°$, which is a (2 0 0) characteristic peak for MS nanoparticles.[38,40] For the MND adsorbent, there was an observed shift of the (2 0 0) diffraction peak to $2\theta = 5°$ with a reduction in the peak height. The presence of broad diffraction peaks further shifted to $2\theta = 21°$ and 28°, suggesting a decrease in the d-spacing of MS nanoparticles in MND adsorbent due to the incorporation of ND in it.[40] The XRD pattern of ND has been previously described by Omorogie et al.[7]

Also, the XRD pattern of GO nanoparticles showed a tiny peak around $2\theta = 9°$ and 11° due to the presence of abundant oxygen functional groups [21] and another

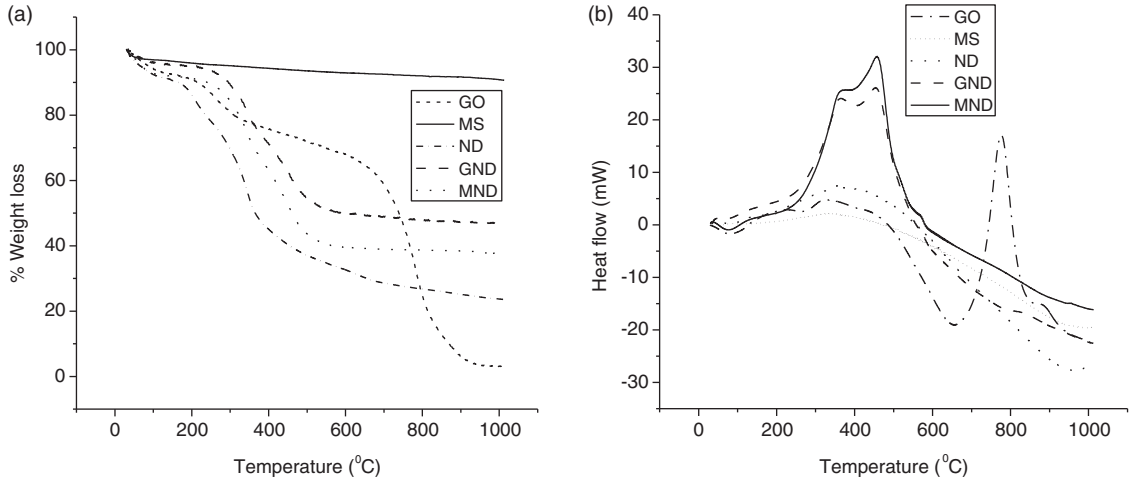

Figure 2. (a) TG analytical profiles for GO and MS nanoparticles, ND agro-waste, GND and MND adsorbents and (b) differential thermal analytical profiles for GO and MS nanoparticles, ND agro-waste, GND and MND adsorbents.

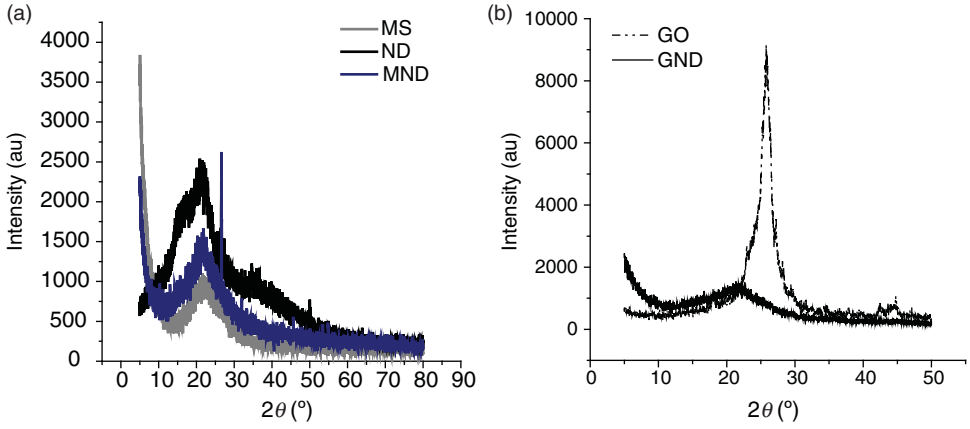

Figure 3. (a) XRD patterns for MS nanoparticles, ND agro-waste and MND adsorbent, and (b) XRD patterns for GO nanoparticles and GND adsorbent.

(0 0 2) peak around $2\theta = 26.2°$.[21] For the GND adsorbent, the (0 0 2) peak found in GO nanoparticles broadened was shifted to $2\theta = 22.9°$ with reduced peak intensity.

3.1.5. *Scanning electron microscopy and transmission electron microscopy*

Figure S1(a), S1(b) andS1(c) shows the SEM images of ND, MS nanoparticles and GO nanoparticles, respectively, while Figure S1(d) and S1(e) shows the TEM images of MS nanoparticles. The SEM image of ND was described by Omorogie et al.[6,7] The SEM image of MS nanoparticles revealed monodispersed array of mesopores on the surface. The SEM image of GO nanoparticles revealed a surface with uneven particles of flower-like structures. The TEM images of MS nanoparticles showed mesopores at 50 nm (see Figure S1 in supplementary material). Figure S2 shows the SEM images of MND and GND adsorbents which suggest that these hybrid materials do have similar particle morphology that are densely packed.

4. Kinetics of adsorption

The experimental data obtained from this study were analysed using the PFO, PSO, DC and HPD kinetic models. The PSO kinetic model gave better linear fits to experimental data of all samples with correlation coefficients $R^2 > 0.999$ (Table 2).

The values of the adsorption capacity, q_e, for Cr(III) and Pb(II) ions adsorption onto GND adsorbent from PSO kinetic model were 7.34 and 7.94 mg/g, respectively, which is 91.95% and 99.25%, respectively, of the total adsorption capacity of the adsorbent if all 20 mg/L of the metal ion were adsorbed (Table 2). This is quite higher than those obtained for ND (69.6% and 77.6% for Cr(III) and Pb(II) ions, respectively), but comparable to those of MND adsorbent (87.8% and 98.9% for Cr(III) and Pb(II) ions, respectively). The increased amounts of Cr(III) and Pb(II) ions uptake by GND and MND adsorbents resulted from an increase in the specific surface area and pore volume of ND after being modified

Table 2. Nonlinear kinetic parameters for the adsorption of Cr(III) and Pb(II) onto ND agro-waste, MND and GND adsorbents.

	ND		MND		GND	
	Cr(III)	Pb(II)	Cr(III)	Pb(II)	Cr(III)	Pb(II)
PFO						
q_e (mg/g)	5.37	6.17	6.87	7.89	7.28	7.94
k_1 (/min)	0.46	0.89	0.60	1.03	0.86	1.45
R^2	0.7684	0.6251	0.6630	0.8238	0.3310	0.5075
PSO						
q_e (mg/g)	5.57	6.21	7.02	7.91	7.34	7.94
k_2 (g/mg min)	0.23	1.61	0.36	3.04	0.93	19.48
h (mg/g min)	7.14	62.09	17.74	190.21	50.10	1228.09
R^2	0.9992	1.0000	0.9993	1.0000	0.9995	1.0000
DC						
q_e (mg/g)	5.57	6.21	7.01	7.91	7.34	7.94
K_{DC} (mg/g.t)	7.13	61.92	17.71	190.53	50.11	1230.91
R^2	0.9992	1.0000	0.9993	1.0000	0.9995	1.0000

with MS nanoparticles and a mixture of GO and MS nanoparticles.

The initial sorption rates h (Table 2), from the PSO kinetic model for the adsorption of Cr(III) and Pb(II) ions by ND increased from 7.14 and 62.09 mg/g min to 17.74 and 190.21 mg/g min, respectively, in MND adsorbent, and 50.10 and 1228.09 mg/g min, respectively, in the GND adsorbent. This increase suggests that the adsorption process was initially very fast, especially the adsorption of Pb(II) ion onto the GND adsorbent (which indicates that as much as 1.228 g of Pb(II) ion was adsorbed per gram of GND every minute). However, the modification of ND with either MS or GO + MS nanoparticles increased the overall rate of removal of Pb(II) ion from the aqueous solution (Table 2).

The addition of GO + MS nanoparticles to ND improved its adsorption capacity but not significantly. However, the modifications increased the rate of removal of Pb(II) ion by MND and GND adsorbents to ≈ 3 times and ≈ 20 times the rate of ND, respectively (Table 2).

It is worthy to note here that the impact of modifying ND with MS + GO nanoparticles was far more on its kinetic property than on its capacity to adsorb these toxic metal ions from aqueous solutions. For large-scale application of this adsorbent (GND), this has strong positive implications and it is attractive as it improves turnover time for the adsorption process. The correlation coefficients (Table 2) showed that kinetic data were better described by the PSO kinetic model compared with others. This is an indication that the main controlling mechanism for the adsorption of these toxic metal ions onto the various adsorbents is basically via chemisorption although intraparticle diffusion could also play a small role.

The nonlinear kinetic modelling of the data using the PFO, PSO, DC and HPD kinetic models was done using the Kyplot version 2.0 software®. Figure 4(a–c) shows the nonlinear model plots for the various kinetic models. The nonlinear regression correlation coefficient (Table 2) showed that experimental data gave better fit to PSO and DC kinetic models (R^2 values shown in Table 2). Results for the adsorption of Cr(III) from PSO, DC and HPD kinetic models suggest that the rate of adsorption of Cr(III) and Pb(II) onto GND adsorbent and the subsequent diffusion coefficient is higher than with other adsorbents (Tables 2 and 3). However, from the HPD kinetic model (Table 3), we observed that the rate of adsorption of Cr(III) via particle diffusion is lower than that through liquid diffusion and that adsorption of Pb(II) via liquid film diffusion was higher than for Cr(III). No result was obtained for adsorption of Pb(II) through the particle diffusion mode because the data

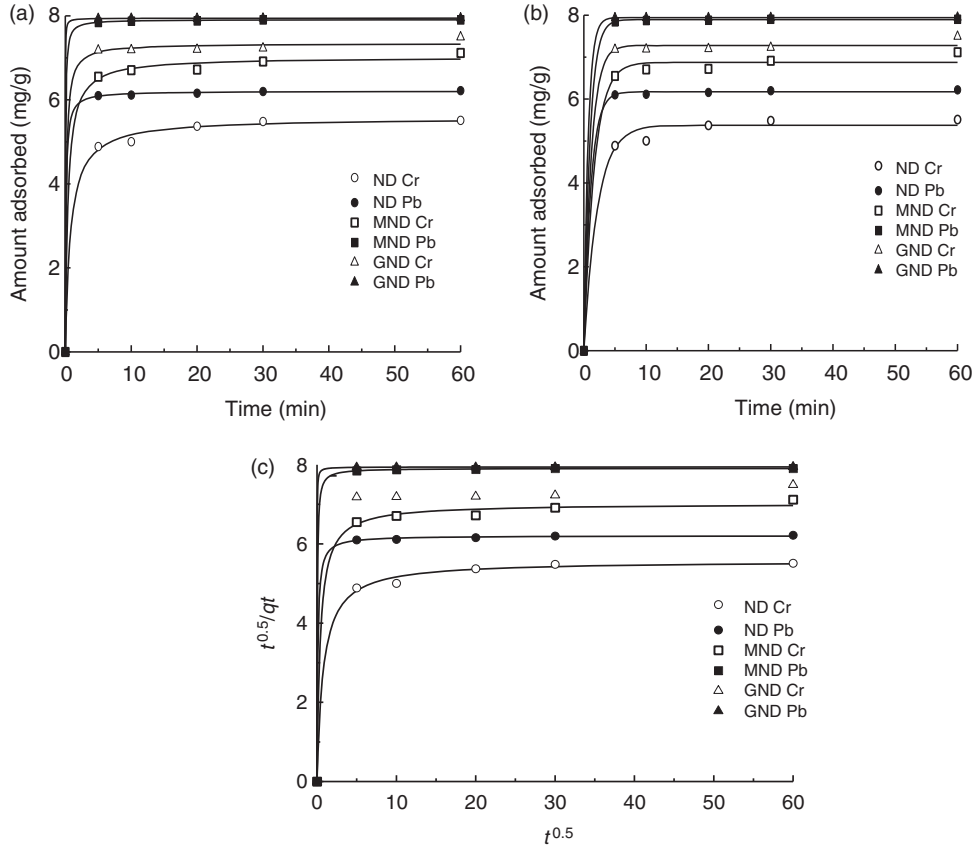

Figure 4. (a) PFO, (b) PSO and (c) DC kinetic model plots for the uptake of Cr(III) and Pb(II) ions onto ND agro-waste, GND and MND adsorbents.

Table 3. Homogeneous particle diffusion model (HPDM) parameters for ND, GND and MND adsorbents.

	K	D_e	r^2	Variance (%)
ND				
Cr(III)				
HPDM L	0.39	2.08×10^{-5}	0.9893	0.16
HPDM P	0.13	8.23×10^{-10}	0.9925	0.11
Pb(II)				
HPDM L	0.77	4.6×10^{-5}	0.9994	9.43×10^{-3}
HPDM P	–	–	–	–
GND				
Cr(III)				
HPDM L	0.62	3.87×10^{-5}	0.9943	0.09
HPDM P	1.00	2.53×10^{-10}	0.9999	0.13
Pb(II)				
HPDM L	1.23	8.15×10^{-5}	0.9999	1.17×10^{-4}
HPDM P	–	–	–	–
MND				
Cr(III)				
HPDM L	0.48	7.14×10^{-6}	0.9906	0.14
HPDM P	0.17	4.05×10^{-11}	0.9916	0.13
Pb(II)				
HPDM L	0.97	1.60×10^{-5}	0.9999	5.78×10^{-4}
HPDM P	–	–	–	–

Note: HPDM, homogeneous particle diffusion model; $k = s^{-1}$; $D_e = m^2\,s^{-1}$.

obtained (raw data not shown) for the adsorption process showed that the reaction was perhaps too fast for the HPD model to analyse.

These results further support our earlier claims that the adsorption of these ions were through diffusion and chemisorption mechanism, although from HPD kinetic model data, the diffusion of ions through the adsorbents (particle diffusion) is the slowest step and hence the rate-determining step. The higher diffusion coefficients and rates of adsorption shown by Pb(II) ion are due to the fact that it has a lower hydration energy and will thus loose its hydration shell more easily and be adsorbed faster than Cr(III) ion.[41,42]

5. Conclusion

This research investigated the use of a new class of hybrid materials from agro-waste and nanomaterials to sequester Cr(III) and Pb(II) ions. The result obtained indicates that very high specific surface area and pore structure of the hybrid materials were responsible for its excellent toxic metal ions uptake capacity with respect to the agro-waste. From PSO, DC and HPD models, it was discovered that the uptake of Cr(III) and Pb(II) ions by GND adsorbent was the fastest of all the adsorption processes. This implies that the industrial application of GND adsorbent for the treatment of effluent will yield very high turnover efficiency for a short period of time. Modification of ND with either MS and MS + GO nanoparticles increased both rate of adsorption and diffusion coefficient for the adsorption of Cr(III) and Pb(II) with the latter modified adsorbent giving better kinetic characteristics. Agro-wastes modified with nanoparticles are potential adsorbents for efficient removal of toxic heavy metal ions from water and wastewater, giving that they are relatively cheap and easy to prepare.

Acknowledgements

The authors acknowledge the support of The World Academy of Sciences for the advancement of science in developing countries and the Chinese Academy of Sciences (TWAS-CAS) for providing fellowship to Martins O. Omorogie at the Laboratory for Nanodevices, National Center for Nanoscience and Technology, Beijing, China where this research was carried out.

Funding

This work was also supported in part by the National Basic Research Program of China (973 Program No. 2011CB933401) and the National Natural Science Foundation of China (21005023). Prof. Jian R. Gong gratefully acknowledges the support of the K.C. Wong Education Foundation, Hong Kong.

Supplemental data

Supplemental data for this article can be accessed http://dx.doi.org/10.1080/09593330.2013.839747.

References

[1] Chiron M, Guilet R, Deydier E. Adsorption of copper (II) and lead (II) onto grafted silica; isotherms and kinetic models. Water Res. 2003;37:3079–3086.
[2] Kotas J, Stasicka Z. Chromium occurrence in the environment and methods of its speciation. Environ Pollut. 2000;107:263–283.
[3] Mathialagan T, Viraraghavan T. Adsorption of cadmium from aqueous solutions by perlite. J Hazard Mater. 2002;94:291–303.
[4] Ho YS, Ofomaja AE. Kinetics and thermodynamics of lead ion sorption on palm kernel fiber from aqueous solution. Process Biochem. 2005;40:3455–3461.
[5] Ho YS, Ofomaja AE. Biosorption thermodynamics of cadmium ion on coconut copra meal as biosorbent. Biochem Eng J. 2006;30:117–123.
[6] Omorogie MO, Babalola JO, Unuabonah EI, Gong JR. Kinetics and thermodynamics of heavy metal ions sequestration onto novel *Nauclea diderrichii* seed biomass. Bioresour Technol. 2012;118:576–579.
[7] Omorogie MO, Babalola JO, Unuabonah EI, Song W, Gong JR. Efficient chromium abstraction from aqueous solution using a low-cost biosorbent: *Nauclea diderrichii* seed waste. J Saudi Chem Soc. In press. Available from: http://dx.doi.org/10.1016/j.jscs.2012.09.017
[8] Unuabonah EI, Olu-Owolabi BI, Taubert A, Omolehin EB, Adebowale KO. SAPK: a novel composite resin for water treatment with very high Zn^{2+}, Cd^{2+} and Pb^{2+} adsorption capacity. Ind Eng Chem Res. 2013;52(2):578–585.
[9] Cao W, Dang Z, Yia X-Y, Yang C, Lu G-N, Liu Y-E, Huang S-Y, Zheng L-C. Removal of chromium(VI) from electroplating wastewater using an anion exchanger derived from rice straw. Environ Technol. 2013;34(1):7–14.
[10] Chen G, Fan J, Liu R, Zeng G, Chen A, Zou Z. Removal of Cd(II), Cu(II) and Zn(II) from aqueous solutions

by live *Phanerochaete chrysosporium*. Environ Technol. 2012;33(23):2653–2659.
[11] Campos I, Alvarez JA, Villar P, Pascual A, Herrero L. Foundry sand as low-cost adsorbent material for Cr(VI) removal. Environ Technol. 2013;34(10):1267–1281.
[12] Chen Y, Hu J, Wang J. Kinetics and thermodynamics of Cu(II) biosorption onto novel magnetic chitosan composite bead. Environ Technol. 2012;33(20):2645–2651.
[13] Kresge CT, Leonowicz ME, Roth WJ, Vartuli JC, Beck JS. A new family of mesoporous molecular sieve prepared with liquid crystal templates. Nature. 1992;359:710–719.
[14] Ying JY, Mehnert CP, Wong MS. Synthesis and application of supramolecular-templated mesoporous materials. Angew Chem Int Ed. 1999;38:56–77.
[15] Vallet-Regí M, Ruiz-González L, Izquierdo-Barba I, González-Calbet JM. Revisiting silica based ordered mesoporous materials: medical applications. J Mater Chem. 2006;16:26–31.
[16] Witula T, Holmberg K. Use of different types of mesoporous materials as tools for organic synthesis. J Colloid Interface Sci. 2007;310:536–545.
[17] Luengo C, Puccia V, Avena M. Arsenate adsorption and desorption kinetics on a Fe(III)-modified montmorillonite. J Hazard Mater. 2011;86:1713–1719.
[18] Mason S, Iceman C, Tanwar K, Trainor T, Chaka A. Pb(II) adsorption on isostructural hydrated alumina and haematite (0001) surfaces: a DFT study. J Phys Chem C. 2009;113:2159–2170.
[19] Ai L, Zhang C, Chen Z. Removal of methylene blue from aqueous solution by a solvothermal-synthesized graphene/magnetite composite. J Hazard Mater. 2011;192: 1515–1524.
[20] Li N, Zheng M, Chang X, Ji G, Lu H, Xue L, Pan L, Cao J. Preparation of magnetic $CoFe_2O_4$-functionalized graphene sheets via a facile hydrothermal method and their adsorption properties. J Solid State Chem. 2011;184:953–958.
[21] Sun L, Yu H, Fugetsu B. Graphene oxide adsorption enhanced by in situ reduction with sodium hydrosulfite to remove acridine orange from aqueous solution. J Hazard Mater. 2012;203–204:101–110.
[22] Hummers WS, Offeman RE. Preparation of graphitic oxide. J Am Chem Soc. 1958;80(6):1339–1339.
[23] Lagergren S. Zur theorie der sogenannten adsorption geloster stoffe. Kungliga SVenska Vetenskapsakademiens. Handlingar Band. 1898;24:1–39.
[24] Azizian S. Kinetic models of sorption: a theoretical analysis. J Colloid Interface Sci. 2004;276:47–52.
[25] Ho YS, McKay G. Pseudo-second order model for sorption processes. Process Biochem. 1999;34(5):451–465.
[26] Sutherland C, Venkobachar C. A diffusion–chemisorption model for simulating biosorption using forest, *Formes fasciatus*. Int Res J Plant Sci. 2010;1(4):107–117.
[27] Wright PR, Muzzio FM, Glasser BJ. Batch uptake of lysozyme: effect of solution viscosity and mass transfer on adsorption. Biotechnol Prog. 1998;56:3149–3162.
[28] Shehata FA, Attallah MF, Borai EH, Hilal MA, Abo-Aly MM. Sorption reaction mechanism of some hazardous radionuclides from mixed waste by impreganated crown ether onto polymeric resin. Appl Radiat Isotopes. 2010;68:239–249.
[29] Haerifar M, Azizian S. Fractal-like adsorption kinetics at the solid/solution interface. J Phys Chem C. 2012;116: 13,111–13,119.
[30] Vermeulen T, Klein G, Hiester NK. Adsorption and ion exchange. New York: McGraw-Hill; 1973.
[31] Zhang X, Wu W, Wang J, Liu C. Evaporation-induced self-assembly of amino-functionalized mesoporous silica thin films by sol–gel process. J Am Ceram Soc. 2007;90(3): 965–968.
[32] Tanev PT, Pinnavaia TJ. Mesoporous silica molecular sieves prepared by ionic and neutral surfactant templating: a comparison of physical properties. Chem Mater. 1996;8: 2068–2079.
[33] Paraknowitsch JP, Zhang Y, Thomas A. Synthesis of mesoporous composite materials of nitrogen-doped carbon and silica using a reactive surfactant approach. J Mater Chem. 2011;21:15,537–15,543.
[34] Fowler CE, Lebeau B, Mann S. Covalent coupling of an organic chromophore into functionalized MCM-41 mesophases by template-directed co-condensation. Chem Commun. 1998;17:1825–1826.
[35] Yang S, Kima IJ, Jeon MJ, Kima K, Moon SI, Kima HS. Preparation of graphite oxide and its electrochemical performance for electric double layer capacitors. J Ind Eng Chem. 2008;14:365–370.
[36] Hao L, Song H, Zhang L, Wan X, Tang Y, Lv Y. SiO_2/graphene composite for highly selective adsorption of Pb(II) ion. J Colloid Interface Sci. 2012;369:381–387.
[37] Gupta S, Babu BV. Utilization of waste product (tamarind seeds) for the removal of Cr(VI) from wastewater: equilibrium, kinetics and regeneration studies. J Environ Manage. 2009;90:3013–3022.
[38] Zarabadi-Poor P, Badiei A, Fahlman BD, Arab P, Ziarani GM. One-pot synthesis of ethanolamine-modified mesoporous silica. Ind Eng Chem Res. 2011;50:10,036–10,040.
[39] Huo Q, Margolese DI, Stucky GD. Surfactant control of phases in the synthesis of mesoporous silica-based materials. Chem Mater. 1996;8:1147–1160.
[40] Lee B, Kim Y, Lee H, Yi J. Synthesis of functionalized porous silicas via templating method as heavy metal ion adsorbents: the introduction of surface hydrophilicity onto the surface of adsorbents. Micro Meso Mat. 2001;50:77–90.
[41] Mobasherpour I, Salahi E, Pazouki M. Comparative of the removal of Pb^{2+}, Cd^{2+} and Ni^{2+} by nano crystallite hydroxyapatite from aqueous solutions: adsorption isotherm study. Arabian J Chem. 2012;5:439–446.
[42] Adie UG, Unuabonah EI, Adeyemo AA, Adeyemi GO. Biosorptive removal of Pb^{2+} and Cd^{2+} onto novel biosorbent: defatted *Carica papaya* seeds. Biom Bioener. 2011;35:2517–2525.